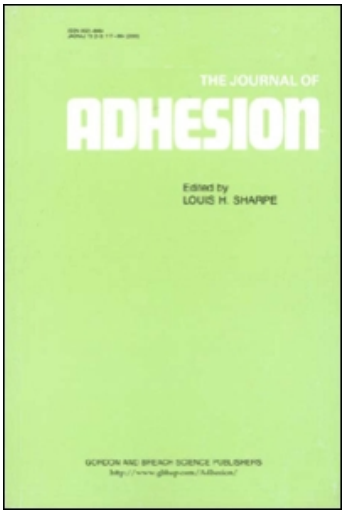

The Journal of Adhesion

Publication details, including instructions for authors and subscription information:
http://www.informaworld.com/smpp/title~content=t713453635

In-Plane Ordering of a Genetically Engineered Viral Protein Cage

Michael T. Klem[ab]; Peter Suci[bc]; David W. Britt[d]; Mark Young[bc]; Trevor Douglas[ab]
[a] Department of Chemistry, Montana State University, Bozeman, MT, USA [b] Center for Bioinspired NanoMaterials, Montana State University, Bozeman, MT, USA [c] Department of Plant Sciences, Montana State University, Bozeman, MT, USA [d] Biological Engineering, Utah State University, Logan, UT, USA

To cite this Article Klem, Michael T. , Suci, Peter , Britt, David W. , Young, Mark and Douglas, Trevor(2009) 'In-Plane Ordering of a Genetically Engineered Viral Protein Cage', The Journal of Adhesion, 85: 2, 69 — 77
To link to this Article: DOI: 10.1080/00218460902781966
URL: http://dx.doi.org/10.1080/00218460902781966

The Journal of Adhesion, 85:69–77, 2009

ISSN: 0021-8464 print/1545-5823 online
DOI: 10.1080/00218460902781966

Taylor & Francis
Taylor & Francis Group

In-Plane Ordering of a Genetically Engineered Viral Protein Cage

Michael T. Klem[1,2], Peter Suci[2,3], David W. Britt[4], Mark Young[2,3], and Trevor Douglas[1,2]
[1]Department of Chemistry, Montana State University, Bozeman, MT, USA
[2]Center for Bioinspired NanoMaterials, Montana State University, Bozeman, MT, USA
[3]Department of Plant Sciences, Montana State University, Bozeman, MT, USA
[4]Biological Engineering, Utah State University, Logan, UT, USA

Protein cages architectures can be used as nanoscale building blocks to fabricate higher order structures. We show here that in-plane ordering can be induced in films of a genetically engineered viral protein cage bound electrostatically to a planar surface. Surface pressure measurements were used to follow the kinetics of adsorption of the virus nanoparticle at the air-water interface for a range of sucrose and nanoparticle subphase concentrations. Atomic force microscope (AFM) images indicated that with optimal subphase conditions films transferred to solid supports exhibited regions of hexagonal packed 2-D arrays. Potential applications of these monolayer assemblies of protein cage architectures include their use as scaffolds to immobilize functional groups at a surface or as templates for building multilayer films.

Keywords: AFM; Air-water interface; Cowpea chlorotic mottle virus; Hexagonal packed arrays; Langmuir-Blodgett; Protein cage; Sucrose

Received 19 August 2008; in final form 29 October 2008.
One of a collection of papers honoring J. Herbert Waite, the recipient in February 2009 of *The Adhesion Society Award for Excellence in Adhesion Science, Sponsored by 3 M.*

Address correspondence to either Mark Young, Department of Plant Sciences & Plant Pathology, 111A CBB, Montana State University, Bozeman, MT 59717, USA. E-mail: myyoung@montana.edu or Trevor Douglas, Department of Plant Chemistry and Biochemistry, 113 CBB, Montana State University, Bozeman, MT 59717, USA. E-mail: tdouglas@chemistry.montana.edu

INTRODUCTION

Protein cages are natural spherical nanoparticles composed of symmetrically arranged monomeric protein subunits [1,2]. Protein cages have been used as targeted delivery vehicles for drugs [3] and imaging agents [4–7], and as spatially defined templates for synthesis of a variety of materials [4,8–16]. From the perspective of fabrication of solid state devices, a protein cage shell enclosing a chosen material is a building block that can be used for assembling higher order structures that determine nanoscale properties of the bulk material [17].

Protein cage architectures have been organized into higher order structures by Au-thiol interactions [18], layer-by-layer assembly [19,20], dip pen lithography [21], complementary biological interactions [22], and three-dimensional crystallization [23]. Adsorption at the air-water interface provides a means to assemble monolayers of protein cages that exhibit in-plane ordering [24,25]. Potential applications of these two-dimensional arrays include interfacial components of sensors, catalytic surfaces, electrochemical, and photovoltaic devices.

Cowpea chlorotic mottled virus (CCMV) is an icosahedral protein cage composed of 180 identical monomeric protein subunits with a diameter of 28 nm [26]. In its natural state, each monomeric subunit projects a disordered N-terminal chain into the interior cavity. Basic residues (6 arg and 3 lys) are thought to stabilize incorporation of its RNA cargo through electrostatic interactions. We designed a genetic construct (subE) in which nine basic residues at the N-terminus were replaced by glutamic acid residues. The subE mutant assembles into a viral cage identical in structure and size to wildtype CCMV and was shown to nucleate the formation of iron oxide nanoparticles selectively in the interior compartment of the protein shell [10]. Here, we show that two-dimensional ordered arrays of an exceptionally stable, cross-linked form of subE (subE X) can be induced to assemble on a positively charged solid support by initially concentrating the virus particle at the air-water interface under optimal subphase conditions.

METHODS

Protein Cage Preparation

The construction of subE, in which nine basic residues at the N-termini (6 arg and 3 lys) were replaced with glutamic acid has been described [10]. SubE was cross-linked (subE X) with glutaraldehyde by reacting a 0.5 mg/mL solution of subE with a 5% solution of glutaraldehyde in 100 mM HEPES (Sigma-Aldrich, St. Louis, MO, USA) buffer at pH 7.0 for 20 h with stirring at room temperature. The

reaction was quenched with 1 M TRIS (pH 7.0) (Sigma-Aldrich). The cross-linked protein was purified by size exclusion chromatography (Superose 6 column, GE Healthcare, Bioscilaces AB, Upsala, Sweden) and dialysis (12–14 kDa membrane). Cross-linked subE (subE X) maintains its structure upon heating to 70°C (data not shown).

Surface Pressure Measurements

Surface pressure changes in 500 μL drops of aqueous solution were measured using a MicroTroughXL tensiometer (Kibron Inc., Espoo, Finland). Aliquots of subE X at 500 μg/mL were injected into the subphase of drops using a Hamilton syringe (Hamilton Syringe, Reno, NY, USA).

Preparation and Characterization of SubE X Films on Solid Supports

Poly-L-lysine (plys) (Sigma-Aldrich) coated Si <100> wafers (Virginia Semiconductor Inc., Fredericksburg, VA, USA) were prepared by adsorbing plys from a 1 mg/mL aqueous solution for 1 h followed by rinsing in nanopure water and drying in a stream of nitrogen.

AFM imaging was performed using tapping mode on a Nanoscope III Multimode SPM (Digital Instruments, Inc., Santa Barbara, CA, USA). The probes used were Tap300 cantilevers (NanoDevices, Santa Barbara, CA, USA). The resultant images were then processed with Nanoscope III (Digital Instruments) and WSxM (Nanotec Electronica, Madrid, Spain) software packages.

RESULTS

Injection of subE X into a water subphase or at the air-water interface produces a transient increase in surface pressure which then relaxes to near baseline levels (Fig. 1). An immediate increase in surface pressure is obtained by merely injecting an aliquot of water containing no subE X into the subphase (Fig. 1a). The presence of subE X in the injected aliquot appears to reduce the rate of decline in surface pressure (Fig. 1b), but there is no indication of a stable change in surface pressure that is maintained above the baseline even upon injection of an additional aliquot containing subE X into the subphase (Fig. 1c). The decline in surface pressure is even more rapid upon injection of an aliquot containing subE X at the air-water interface (Fig. 1d).

Surface pressure changes upon injection of subE X into a 3% sucrose aqueous solution are similar to those obtained in pure water (Fig. 2a). This is in contrast to surface pressure changes upon injection

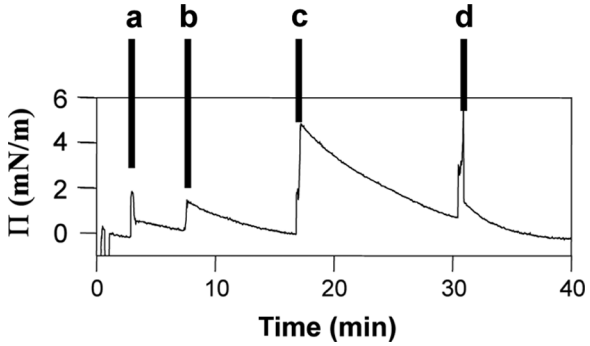

FIGURE 1 Surface pressure changes upon injection of water or subE X into a water subphase or at the air-water interface. a) 20 μL water; b) 20 μL of a 500 μg/mL solution of subE X; c) 50 μL of a 500 μg/mL solution of subE X; d) 30 μL of a 500 μg/mL solution of subE X deposited at the interface.

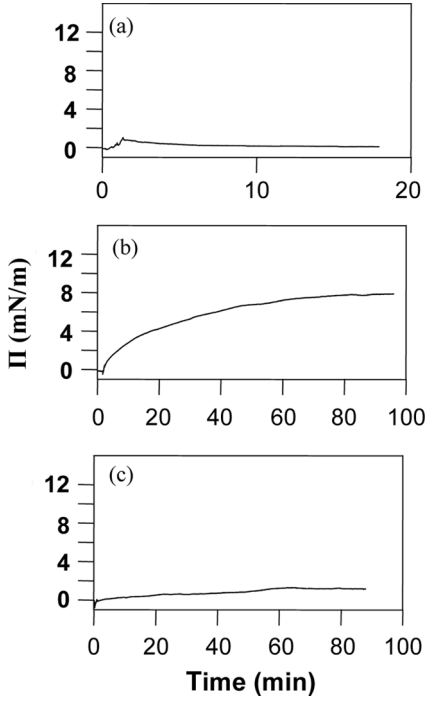

FIGURE 2 Surface pressure changes upon injection of subE X into an aqueous subphase containing sucrose; the subphase concentration of subE X was 50 μg/mL. a) 3% sucrose; b) 5% sucrose; c) 10% sucrose.

of subE X into a subphase of 5% sucrose (Fig. 2b). In this case, the surface pressure rises, eventually reaching a plateau value of approximately 8 mN/m. This trend is reversed if more sucrose is added to the subphase. Injection of subE X into a 10% sucrose solution results in a slight gradual increase in surface pressure that plateaus at approximately 1 mN/m (Fig. 2c).

The kinetics of surface pressure changes upon injection of subE X into a subphase containing 5% sucrose were measured for a range of different subE X concentrations (Fig. 3a). The data curves were quantified by fitting the data to a first order rate equation:

$$\Pi(t) = k(1 - \exp(rt)), \tag{1}$$

where Π is surface pressure, t is time, r is the rate constant (min^{-1}), and k is the projected plateau value for long times. Values for r and k are presented in Figs. 3b and c, respectively.

We interpret the changes in surface pressure as reflecting adsorption of subE X at the air-water interface. The alternative possibility

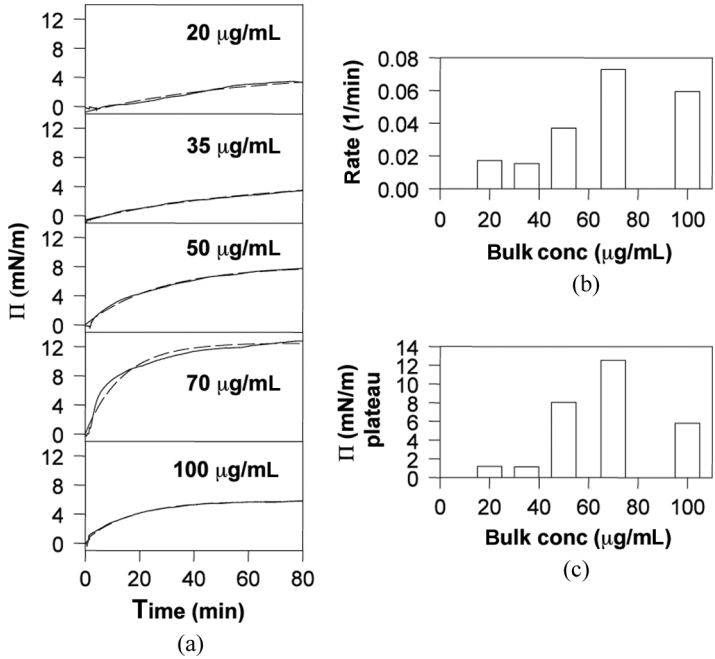

FIGURE 3 Influence of subphase concentration of subE X on the rate and extent of adsorption from a 5% sucrose aqueous solution; a) Fits (broken lines) of Eq. (1) to the data curves (solid lines); b) rate constants for adsorption; c) projected surface pressures for infinite time.

that surface active contaminants are producing the changes in surface pressure is unlikely since subE X was purified by both size exclusion chromatography and extensive dialysis. In addition, there is no evidence of adsorption of surface contaminants at the air-water interface under the conditions used to obtain the results presented in Fig. 1. Based on this interpretation, the data indicate that both the rate and extent of adsorption were maximum at a subphase concentration of 70 μg/mL.

Using results presented in Figs. 3b and c as a guide, we attempted to transfer subE X adsorbed at the air-water interface to a positively charged solid support using horizontal transfer from the air side. We found previously that irreversible adsorption of CCMV onto a solid support from an aqueous solution can be driven by electrostatic interactions [27]. The subphase was 5% sucrose and the subphase concentration was 70 μg/ml. After transfer, $1 \times 1\,\mu m^2$ areas on the surface were examined using AFM. A representative image is shown in Fig. 4. All locations on the film clearly exhibited regions of hexagonally packed virus particles. There were also regions where the monolayer structure was disrupted, either by formation of multilayers or absence

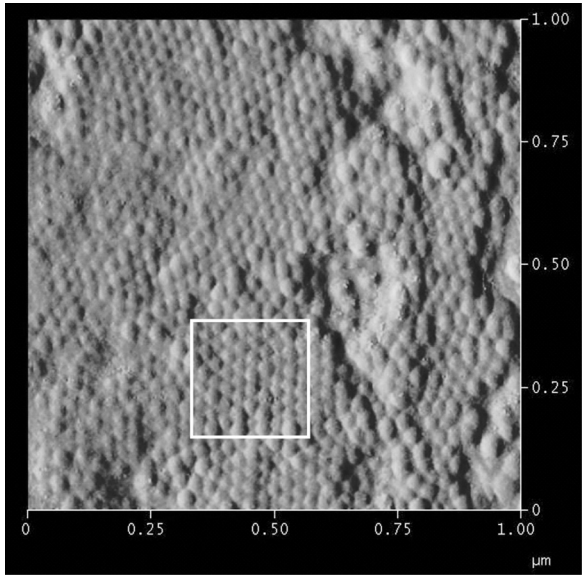

FIGURE 4 AFM image of a densely packed film of subE X transferred to a p-lys coated Si solid support from a 70 μg/mL subE X aqueous solution in 5% sucrose. The image size is 1 μm × 1 μm. The white bounded square highlights a region of hexagonally packed viral nanoparticles.

of transfer. We are presently fine tuning conditions to attempt to obtain films in which hexagonal close packing is extended over a longer range.

DISCUSSION

We showed previously that the areal surface coverage of CCMV obtained by adsorption from solution and driven by electrostatic interactions was limited to less than 54.7% in accordance with the random sequential adsorption (RSA) model [27]. Using the air-water interface to first concentrate the nanoparticles and then transferring them to a solid support *via* electrostatic interactions nearly doubles the surface coverage (90.6% for a hexagonally packed array). This has significant implications for surface modification using mono or multilayer films of CCMV or genetic CCMV constructs. In addition, the induction of adsorption at the air-water interface by sucrose is useful since it allows assembly of a hexagonally packed film that consists only of the virus particle with no surface active additives.

We attribute the formation of hexagonal packed arrays to a combination of the particles' affinity for the air-water interface and their mobility at that interface. Ordering of CCMV into both hexagonal and square arrays has been demonstrated on freshly cleaved mica [28]. In this case, the self-organization into ordered arrays was attributed to substrate-induced epitaxial growth.

The influence of sucrose on adsorption at the air-water interface is interesting from a fundamental perspective. Although the greater density of 5% sucrose (1.018) compared with water may enhance adsorption by increasing the buoyancy of the virus particles, this cannot explain the phenomenon since the buoyant density of the virus is between 1.356 and 1.383 [26]. In addition, if an increase in the buoyancy of the virus was a significant factor then adsorption should be more pronounced at 10% sucrose than at 5% sucrose. It is unlikely that the influence of sucrose depends on specific molecular properties of the virus particle since osmolytes also enhance adsorption of other protein cages (ferritin [25,29]) and proteins (bovine serum albumin [30]) at the air-water interface.

It is possible that preferential hydration of the protein cage conferred by sucrose makes adsorption at the air-water interface energetically favorable, although we cannot provide a comprehensive explanation. Co-solvents such as sugars and polyols are known to stabilize proteins *via* a mechanism whereby the co-solvent is excluded from the protein surface [31]. As a consequence, the protein tends to retain its conformation. It may be that the loss of the structured

water/protein preferential hydration shell that accompanies adsorption at the air-water interface is sufficient to drive the process entropically.

CONCLUSIONS

We have demonstrated that control of sucrose and viral particle concentrations in the subphase was vital for the formation of hexagonally closed packed arrays at the air-water interface. Horizontal transfer of these ordered arrays to a positively charged Si substrate was also performed. These observations have clear implications for the creation of ordered viral films to be used in applications ranging from sensors to recording media.

ACKNOWLEDGMENTS

This research was supported in part by grants form the National Science Foundation (CBET-0709358), Office of Naval Research (N00014-03-1-0692), and the Department of Energy (DE-FG02-07ER46477).

REFERENCES

[1] Uchida, M., Klem, M. T., Allen, M., Suci, P., Flenniken, M., Gillitzer, E., Varpness, Z., Liepold, L. O., Young, M., and Douglas, T., *Adv. Mater.* **19**, 1025–1042 (2007).
[2] Douglas, T. and Young, M., *Science* **312**, 873–875 (2006).
[3] Flenniken, M. L., Liepold, L. O., Crowley, B. E., Willits, D. A., Young, M. J., and Douglas, T., *Chem. Comm.* 447–449 (2005).
[4] Allen, M., Bulte, J. W. M., Liepold, L., Basu, G., Zywicke, H. A., Frank, J. A., Young, M., and Douglas, T., *Magn. Reson. Med.* **54**, 807–812 (2005).
[5] Uchida, M., Flenniken, M. L., Allen, M., Willits, D. A., Crowley, B. E., Brumfield, S., Willis, A. F., Jackiw, L., Jutila, M., Young, M. J., and Douglas, T., *J. Am. Chem. Soc.* **128**, 16626–16633 (2006).
[6] Flenniken, M. L., Willits, D. A., Harmsen, A. L., Liepold, L. O., Harmsen, A. G., Young, M. J., and Douglas, T., *Chem. Biol.* **13**, 161–170 (2006).
[7] Liepold, L., Anderson, S., Willits, D., Oltrogge, L., Frank, J. A., Douglas, T., and Young, M., *Magn. Reson. Med.* **58**, 871–879 (2007).
[8] Allen, M., Willits, D., Mosolf, J., Young, M., and Douglas, T., *Adv. Mater.* **14**, 1562–1565 (2002).
[9] Allen, M., Willits, D., Young, M., and Douglas, T., *Inorg. Chem.* **42**, 6300–6305 (2003).
[10] Douglas, T., Strable, E., Willits, D., Aitouchen, A., Libera, M., and Young, M., *Adv. Mater.* **14**, 415–418 (2002).
[11] Douglas, T. and Young, M., *Nature* **393**, 152–155 (1998).
[12] Douglas, T. and Young, M., *Adv. Mater.* **11**, 679–681 (1999).
[13] Klem, M. T., Resnick, D. A., Gilmore, K., Young, M., Idzerda, Y. U., and Douglas, T., *J. Am. Chem. Soc.* **129**, 197–201 (2007).

[14] Klem, M. T., Willits, D., Solis, D. J., Belcher, A. M., Young, M., and Douglas, T., *Adv. Funct. Mater.* **15**, 1489–1494 (2005).
[15] Klem, M. T., Mosolf, J., Young, M., and Douglas, T., *Inorg. Chem.* **47**, 2237–2239 (2008).
[16] Klem, M. T., Young, M., and Douglas, T., *J. Mater. Chem.* **18**, 3821–3823 (2008).
[17] Dujardin, E. and Mann, S., *Adv. Mater.* **14**, 775–788 (2002).
[18] Klem, M. T., Willits, D., Young, M., and Douglas, T., *J. Am. Chem. Soc.* **125**, 10806–10807 (2003).
[19] Lvov, Y., Haas, H., Decher, G., Mohwald, H., Mikhailov, A., Mtchedlishvily, B., Morgunova, E., and Vainshtein, B., *Langmuir* **10**, 4232–4236 (1994).
[20] Suci, P. A., Klem, M. T., Arce, F. T., Douglas, T., and Young, M., *Langmuir* **22**, 8891–8896 (2006).
[21] Smith, J. C., Lee, K. B., Wang, Q., Finn, M. G., Johnson, J. E., Mrksich, M., and Mirkin, C. A., *Nano Lett.* **3**, 883–886 (2003).
[22] Strable, E., Johnson, J. E., and Finn, M. G., *Nano Lett.* **4**, 1385–1389 (2004).
[23] Falkner, J. C., Turner, M. E., Bosworth, J. K., Trentler, T. J., Johnson, J. E., Lin, T. W., and Colvin, V. L., *J. Am. Chem. Soc.* **127**, 5274–5275 (2005).
[24] Matsumoto, M., *Langmuir* **10**, 3922–3925 (1994).
[25] Okuda, M., Kobayashi, Y., Suzuki, K., Sonoda, K., Kondoh, T., Wagawa, A., Kondo, A., and Yoshimura, H., *Nano Lett.* **5**, 991–993 (2005).
[26] Bancroft, J. B., Hiebert, E., Rees, M. W., and Markham, R., *Virology* **34**, 224–239 (1968).
[27] Suci, P. A., Klem, M. T., Douglas, T., and Young, M., *Langmuir* **21**, 8686–8693 (2005).
[28] Horne, R. W., Hobart, J. M., and Pasqualironchetti, I., *J. Ultrastruct. Res.* **53**, 319–330 (1975).
[29] Yoshimura, H., Scheybani, T., Baumeister, W., and Nagayama, K., *Langmuir* **10**, 3290–3295 (1994).
[30] Nino, M. R. R. and Patino, J. M. R., *Ind. Eng. Chem. Res.* **41**, 1489–1495 (2002).
[31] Shimizu, S. and Smith, D. J., *J. Chem. Phys.* **121**, 1148–1154 (2004).